Intrinsic switching of polarization vortex in ferroelectric nanotubes

Jie Wang* and Marc Kamlah

Forschungszentrum Karlsruhe, Institute for Materials Research II

Postfach 3640, 76021 Karlsruhe, Germany

Abstract

The response of polarization vortex in ferroelectric nanotubes under different levels of curled electric fields is studied by using the phase field method. A critical curled electric field is found, at which the switching of polarization vortex takes place. The vortex switching initiates through the formation of local vortices near the outer surface with the highest energy density. The new vortex grows and the old one shrinks with the motion of local vortices between them. The coexistence of new vortex with original vortex in ferroelectric nanotubes is completely different from that in ferroelectric nanodisks where the coexistence never occurs. It is also found that the interplay between polarizations and strains first retards the nucleation of new vortex. However, once the new vortex appears, the interplay becomes the main driving force for the growth of new vortex.

* Corresponding author. Tel: +49 7247 82 5857, Fax: +49 7247 82 2347.
E-mail address: jie.wang@imf.fzk.de

Ferroelectric nanostructures are attracting considerable attention due to their unusual physical properties and potential applications in memory devices and nanoelectromechanical systems (NEMS) [1-3]. The properties of ferroelectric materials in nanometer scale are substantially different from those of their bulk counterparts. One of the most distinguished properties in nanoferroelectrics is the formation of a new order, i.e. the polarization vortex, because of the strong depolarization field [1]. The vortex states are bistable and can be switched from one state to the other, which holds a promise to increase the density of ferroelectric nonvolatile random access memories by several orders of magnitude. The switching of polarization vortex may be realized through a curled electric field induced by a time-dependent magnetic field via $\nabla \times \mathbf{E}_{curl} = -\partial \mathbf{B} / \partial t$ [4]. What's the minimal curled electric field that could switch the polarization vortex? The answer to this question will be crucial for the application of polarization vortex in future nonvolatile random access memories. To our knowledge, this issue has not been studied before.

Another important and interesting topic in the field is the switching mechanism of defect-free polarization vortex. Due to the small size, ferroelectric nanostructures have less structure defects (vacancies, dislocations, etc.). These defects are often the nucleation sites of new domains in bulk ferroelectric materials [5]. Even in the absence of a structure defect, some ferroelectric nanostructures (such as dots, disks and rods) still have an intrinsic topological defect at the vortex core due to their geometry constraints. Near the vortex core, the shape change of polarization will induce large strain energy through the coupling between the polarization and the strain. The vortex center will be the nucleation center for a new vortex under a curled electric field [4]. Ferroelectric nanotubes (FNTs), which received much attention recently [6-8], have the same topology as a core-free vortex structure. Recent phase field simulations show that the polarizations in ferroelectric nanotubes form a perfect vortex structure without any intrinsic topological defects [9]. Thus, ferroelectric nanotubes are

suitable candidates for the investigation of the switching mechanism of defect-free polarization vortex under curled electric fields.

Most previous works assumed the polarization switching of ferroelectrics as a thermally activated nucleation process [10, 11]. According to the Landauer paradox, the small thermal fluctuation energy can not surpass the implausibly large nucleation activation energy [12]. Despite about half a century of extensive theoretical and experimental effort, the microstructural origins of the Landauer paradox are still poorly understood [13]. Recent experiments show that the highly concentrated electric field induced by the piezoresponse force spectroscopy (PFS) makes the polarization switching in single domains close to the intrinsic thermodynamic limit [14, 15]. Although the switching mechanism in PFS is different from the traditional planar capacitor cases, the opposite domains still nucleate from the surface or from atomic scale defects. For both the planar capacitor and PFS cases, the normal polarization component is nonzero and discontinuous on the surface. New domains often nucleate from the surface. For the polarization vortex in ferroelectric nanotubes, the polarization vectors form perfect closed loops in annular direction, which makes the polarizations continuous along the vortex direction. Therefore, the polarization switching of defect-free ferroelectric vortex under curled fields is significantly more complex than those of planar capacitor and PFS cases.

In this letter, we perform phase field simulations to investigate for the first time the intrinsic switching of a defect-free polarization vortex in ferroelectric $PbTiO_3$ nanotubes subjected to a curled electric field. The phase field simulations are based on the time-dependent Ginzburg-Laudau equation, mechanical equilibrium equation and Gauss' law. In the phase field approach, the total free energy of a ferroelectric system is obtained by integrating the Helmholtz free energy density over the whole volume. The Helmholtz free

energy density ψ is related to the electrical (Gibbs) enthalpy density h by the Legendre transformation $h = \psi - \mathbf{D}\cdot\mathbf{E}$, where $\mathbf{D}$ and $\mathbf{E}$ are electric displacement and electric field, respectively. The electrical enthalpy is a function of polarization $\mathbf{P}$, strain $\boldsymbol{\varepsilon}$, polarization gradient $\nabla\cdot\mathbf{P}$ and electric field $\mathbf{E}$, which can be expressed as [16-18]

$$h = f_{Lan}(\mathbf{P}) + f_{Ela}(\boldsymbol{\varepsilon}) + f_{Cou}(\mathbf{P},\boldsymbol{\varepsilon}) + f_{Gra}(\nabla\cdot\mathbf{P}) + f_{Ele}(\mathbf{E},\mathbf{P}) . \quad (1)$$

The first term on the right hand side of Eq. (1) represents the Landau-Devonshire free energy density. The second and third terms are the elastic energy density and the coupling energy density between the strain and the polarization. The fourth term is the gradient energy, which is attributed to the spatially inhomogeneous polarization. The last term is the electric energy density due to the presence of the electric field. In the present study, we extended the electric field $\mathbf{E}$ in Eq.(1) to include the uncurled electric field $\mathbf{E}^{Unc}$ generated by the inhomogeneous polarizations (the depolarization field) and a prescribed curled electric field $\mathbf{E}^{Cur}$, i.e., $\mathbf{E} = \mathbf{E}^{Unc} + \mathbf{E}^{Cur}$. The same curled electric field as Ref.[4], i.e., $\mathbf{E}^{Cur} = \frac{1}{2}\mathbf{S}\times\mathbf{r}$, is employed here, where $\mathbf{S}$ is the vorticity vector of the curled field. The vorticity vector $\mathbf{S}$ is thermodynamically conjugated field to the toroidal moment of polarization $\mathbf{G}$, which is defined as $\mathbf{G} = \frac{1}{V}\int_V \mathbf{r}\times\mathbf{P}\,dV$. With the presence of different vortices $\mathbf{S}$, the toroidal moment $\mathbf{G}$ will change correspondingly.

The temporal evolution of the polarization in ferroelectric nanotubes is obtained from the following time-dependent Ginzburg-Landau equation

$$\frac{\partial P_i(\mathbf{r},t)}{\partial t} = -L\frac{\delta F}{\delta P_i(\mathbf{r},t)} \quad (i=1, 2, 3), \quad (2)$$

where L is the kinetic coefficient, $F = \int_V \psi\, dv$ is the total free energy of the simulated system, $\delta F / \delta P_i(\mathbf{x},t)$ represents the thermodynamic driving force for the spatial and temporal

evolution of the simulated system. In addition to Eq. (2), the mechanical equilibrium equation $\sigma_{ij,j}=0$ and Gauss' law $D_{i,i}=0$ must be simultaneously satisfied for charge-free and body-force-free ferroelectric materials, in which the stress and electric displacement are derived from $\sigma_{ij}=\partial h/\partial \varepsilon_{ij}$ and $D_i=-\partial h/\partial E_i$, respectively. We assume that the ferroelectric nanotubes are freestanding and open-circuited. The corresponding mechanical and electrical boundary conditions are $\sigma_{ij}n_j=0$ and $D_i n_i=0$, respectively, where n_j denotes the component of unit vector normal to the surface. The free boundary condition of $\partial P/\partial n=0$ is used for the polarizations on the surfaces [19]. The backward Euler scheme and a nonlinear finite element method are employed for the time integration and spatial discretization, respectively, to solve the time-dependent Ginzburg-Laudau equation, mechanical equilibrium equation and Gauss' law. In the simulations, we employ 4000 discrete brick elements to model the FNTs with 10 elements in the longitudinal direction (in the x_3 axis direction), 40 elements in the annular direction and 10 elements in the radial direction. The longitudinal length of the simulated FNTs is 3nm, and the inner and outer radii are 4 nm and 8 nm, respectively. All the material constants used in the simulation are the same as those in Ref. [20]. For convenience, we normalize all material parameters as in Refs.[21, 22] and solve the normalized equations. Then the normalized solutions without units are transferred to the non-normalized quantities with units based on the normalization formula.

The prescribed vorticity vector of the curled field is assumed as $\mathbf{S}=S\mathbf{e}_3$, where $\mathbf{e}_3$ denotes the unit direction vector of the x_3 axis. The symmetry axis of the nanotube coincides with the x_3 axis, which is parallel to the crystallographic [001] direction. Figure 1 shows the response of toroidal moment $\mathbf{G}$ to a cycling vorticity $\mathbf{S}$ at room temperatures. In the absence of a curled electric field, i.e., $\mathbf{S}=0$, the polarizations form a pure vortex structure as shown by the insert at the center of Fig.1, in which the vortex axis coincides with the

symmetry axis of the nanotube. The polarization vortex is clockwise and thus generates a toroidal moment $\mathbf{G}$ in the x_3 negative direction with the value of -2.95 e/ Å as shown by point A in Fig.1. There is no toroidal moment component in the x_1 and x_2 directions because all the polarization components in x_3 direction are zero. From point A to B in Fig.1, a counterclockwise curled electric field (corresponding to a positive vorticity) is applied with an increment of 0.0325 mV/Å^2. It is found that the magnitude of the toroidal moment decreases gradually but the vortex structure remains unchanged. At each loading point, we let the polarization vortex reach its steady state. When the vorticity of curled electric field increases from 0.23 to 0.26 mV/Å^2, the switching of polarization vortex takes place. As a result, the toroidal moment changes from -2.39 to 3.24 e/ Å as shown from point B to C in Fig.1. For the $Pb(ZrTi)O_3$ nanodisk in Ref. [4], the polarization vortex can be switched under a curled electric field of 0.25 mV/Å^2, which is close to 0.26 mV/Å^2 in the nanotube. Although the present model is different from that of Ref.[4], the physical quantities obtained from two models are comparable. The toroidal moment per unit cell is about 60 e/Å^2 in the nanodisk after switching, while it is calculated to be 3.24 e/ Å$\times$64 Å^3=207.36 e/Å^2 in the nanotube. The toroidal moment of the tube is about three times larger than that of the disk. This is consistent with the fact that the average distance from unit cells to the centers of the tube (12 nm) is about three times larger than that of the disk (3.8 nm). Figure 2(a) and 2(b) give the polarization vortices before and after switching, respectively, corresponding to the switching from point B and C in Fig.1. Before switching, polarizations form a clockwise vortex with a negative toroidal moment. After switching, the polarizations form a counterclockwise vortex in which all the polarizations align along the curled electric field. The contour legend shows different magnitudes of polarizations in different colors. It shows that the polarization magnitude before switching is smaller than that after switching. Interestingly, the

polarizations near the inner surface are smaller than those near the outer surface for both before and after switching.

As the vorticity **S** further increases from 0.26 to 0.325, and to 0.39 mV/Å^2, the magnitude of toroidal moment increases to 3.30, and to 3.35 e/ Å, respectively, while the vortex structure remains counterclockwise. We stop to increase the vorticity at 0.3 (point D), and begin an unloading process by decreasing the vorticity from 0.39 mV/Å^2 to 0. It is found that the toroidal moment doesn't go back along the original path D-C-B-A but follows a new path D-C-E. The polarization vortex reaches another stable state at point E without vorticity, which is different from the original stable state at point A. When a negative vorticity is applied from 0 to -0.39 mV/Å^2, the toroidal moment follows the path E-F-G-H. One can find the switching of the toroidal moment takes place again from points F to G when the negative vorticity changes from -0.23 to -0.26 mV/Å^2. As the negative vorticity recovers from -0.39 mV/Å^2 to 0, the toroidal moment restores to the original state at point A following the path H-G-A. Finally, a symmetrical and rectangular-like hysteresis loop between **G** and **S** is obtained for ferroelectric nanotubes.

Figures 2 (c) and 2 (d) show the energy density in the middle plane of the tube at $x_3 = 1.5$ nm for the vortex states in Figs. 2 (a) and 2 (b), respectively, under the vorticity of 0.26 mV/Å^2. For both cases, the energy densities are highly inhomogeneous but spatial distributions are totally different. Before switching, the highest energy density is located at four intersections between the diagonals of the $x_1 - x_2$ plane and the outer surface of the tube as shown in Fig.2 (c). Figure 3 shows snapshots of local polarization distributions corresponding to the different evolution times during switching from point B to C in Fig.1. The polarizations in the area with higher energy density first decrease in magnitude while orientation remain unchanged as shown in Fig.3 (a). As the evolution time increases, some

polarizations near the outer surface reverse and become aligned along the curled electric field as shown in Fig.3 (b). The locations of the reversed polarizations in Fig.3 (b) coincide with the highest energy density in Fig.2 (c). This result suggests that the new vortex nucleates at the locations with highest energy density. The absence of thermal fluctuation in phase field model means the nucleation is thermodynamically intrinsic. It is interesting that the nucleation process takes place through the formation of four embedded local vortices, which are shown by four ellipses in Fig.3 (b). When the evolution time increases to t/t_0=6.6, the local vortices move towards the inner surface as shown in Fig.3 (c). This makes the polarizations near the outer surface form a new vortex opposite to the original vortex. With the evolution time further increasing, the new vortex grows and the old vortex shrinks through the motion of the local vortices as shown in Fig.3 (d) and 3(e). At the evolution time t/t_0=8.0, the old vortex vanishes and the switching process is completed. The coexistence of the new vortex $-\mathbf{G}$ and original vortex $\mathbf{G}$ in Fig.3 (c) and 3(d) suggests that the domain coexistence mechanism is still valid for toroidal moment switching in defect-free ferroelectric nanotubes. This is completely different from that of ferroelectric nanodisks with topological defect, in which the $-\mathbf{G}$ and $\mathbf{G}$ vortices never coexist [4]. We attribute the difference to the absence of topological defect in nanotubes. The topological defect in nanodisks is the nucleation center for the lateral vortex which acts as a bridge between the $-\mathbf{G}$ and $\mathbf{G}$ states.

Figure 4 (a) shows the change of energies during switching. The total free energy, shown by the curve with solid circles, is obtained by integrating the Helmholtz free energy density over the whole volume. The Helmholtz free energy density is important because it contains information on energy barriers for switching. The total free energy curve shows that the highest energy barrier occurs at t/t_0=6.6. Unlike in nanodisks [4], there is no local energy *valley,* due to the absence of the perpendicular toroidal moment, during the whole switching process in nanotubes. After switching, the magnitudes of in-plane polarizations P_1 and P_2

become larger as shown in Fig.4 (b). The larger polarizations in the vortex structure imply a larger elastic energy because of the larger lattice distortion. This is the reason why the elastic energy after switching are larger than before switching as shown by the curve with upper triangles in Fig.4 (a). The gradient energy is relatively small compared to other energies both before and after switching. It is interesting to find that the coupling energy between the polarization and strain, represented by the curve with lower triangles in Fig.4 (a), increases before t/t_0=6.6. According to Fig.3 (c), the new vortex is formed at t/t_0=6.6. After this point the coupling energy decreases dramatically. This result suggests that the interplay between polarizations and strains first retards the nucleation of new vortex. However, once the new vortex is formed, the interplay becomes the main driving force for the growth of new vortex. The curve with solid triangles in Fig.4 (b) shows the polarization component in the x_3 direction is always zero, which indicates there is no lateral vortex during switching.

To conclude, we investigate the intrinsic switching mechanism of polarization vortices in ferroelectric nanotubes subjected to curled electric fields. The vortex switching takes place through the nucleation of local vortices when the curled electric field exceeds a critical value. The new vortex grows and the old one shrinks with the motion of local vortices between them, which is different from the traditional domain wall motion. It is also found that the interplay between polarizations and strains plays different roles in the different phases of switching. The interplay first retards the nucleation of the new vortex. However, once the new vortex appears, the interplay becomes the main driving force for the growth of new vortex. The coexistence of a new vortex $-\mathbf{G}$ domain and the original vortex $\mathbf{G}$ during the switching suggests that the domain coexistence mechanism is still valid for the toroidal moment switching in defect-free ferroelectric nanotubes. This is completely different from that of ferroelectric nanodisks with topological defect, in which the $-\mathbf{G}$ and $\mathbf{G}$ vortices never coexist [4]. We attribute the difference to the absence of topological defects in nanotubes. The

topological defect in nanodisks is the nucleation center for the lateral vortex which acts as a bridge between $-\mathbf{G}$ and $\mathbf{G}$ states. The response of the toroidal moment to a cycling curled electric field shows a symmetrical and rectangular-like hysteresis loop, which suggests that the polarization vortex in ferroelectric nanotubes has the potential application in future nonvolatile random access memories.

Acknowledgements

JW gratefully acknowledges the support from the Alexander von Humboldt Foundation.

References

[1] I. Naumov, L. Bellaiche, and H. Fu, Nature (London) **432**, 737 (2004).

[2] C. Ahn, K. Rabe, and J. Triscone, Science **303**, 488 (2004).

[3] I. Ponomareva, L. Bellaiche, and R. Resta, Phys. Rev. Lett. **99**, 227601 (2007).

[4] I. Naumov, and H. Fu, Phys. Rev. Lett. **101**, 197601 (2008).

[5] M. E. Lines and A. M. Glass, *Principles and Applications of Ferroelectrics and Related Materials*, (Clarendon, Oxford, 1977).

[6] J. F. Scott, H.J. Fan, S. Kawasaki, J. Banys, M. Ivanov, A. Krotkus, J. Macutkevic, R. Blinc, V. V. Laguta, P. Cevc, J. S. Liu and A. L. Kholkin, Nano Letters **8**, 4404 (2008).

[7] Y. Luo, I. Szafraniak, N.D. Zakharov, V. Nagarajan, M. Steinhart, R.B. Wehrspohn, J.H. Wendorff, R. Ramesh, and M. Alexe, Appl. Phys. Lett. **83**, 440 (2003).

[8] J. Kim, S.A. Yang, Y.C. Choi, J.K. Han, K.O. Jeong, Y.J. Yun, D.J. Kim, S.M. Yang, D. Yoon, H. Cheong, K.S. Chang, T. W. Noh and S.D. Bu, Nano Letters **8**, 1813 (2008).

[9] J. Wang, and M. Kamlah, Appl. Phys. Lett. **93,** 042906 (2008).

[10] A. N. Morozovska, S.V. Svechnikov, E. A. Eliseev, S. Jesse, B.J. Rodriguez, and S. Kalinin, J. Appl. Phys. **102**, 114108 (2007).

[11] A.Y. Emelyanov, Phys. Rev. B 71, 132102 (2005).

[12] Landauer R., J. Appl. Phys. **28** 227 (1957).

[13] Jesse S. B.J. Rodriguez, S. Choudhury, A.P. Baddorf, I.Vrejoiu, D. Hesse, M. Alexe, E.A. Eliseev, A.N. Morozovska, J. Zhang, L.Q. Chen, and S.V. Kalinin, Nature Materials, **7**, 209 (2008).

[14] P. Maksymovych, S. Jesse, M. Huijben, R. Ramesh, A. Morozovska, S. Choudhury, L.Q. Chen, A.P. Baddorf, and S.V. Kalinin, Phys. Rev. Lett. **102**, 017601 (2009).

[15] S.V. Kalinin, B.J. Rodriguez, S. Jesse, Y.H. Chu, T. Zhao, R. Ramesh, S. Choudhury, L.Q. Chen, E.A. Eliseev, and A.N. Morozovska, PNAS, **104**, 20204, (2007).

[16] W.Cao, and L. Cross, Phys. Rev. B **44**, 5 (1991).

[17] S. Nambu, and D Sagala, Phys. Rev. B **50**, 5838 (1994).

[18] Y. Su, and C.M. Landis, J. Mech. Phys. Solids **55**, 280 (2007).

[19] Vendik, and S. Zubko, J. Appl. Phys. **88**, 5343 (2000).

[20] J. Wang, and M. Kamlah, Appl. Phys. Lett. **93,** 262904 (2008).

[21] J. Wang, S.Q. Shi, L.Q. Chen, Y.L. Li, and T.Y. Zhang, Acta. Mater. **52**, 749 (2004).

[22] Y.L. Li, S.Y. Hu, Z.K. Liu, and L.Q. Chen, Acta. Mater. **50**, 395 (2002).

Figure captions

Fig.1 (Color online) The hysteresis loop between the toroidal moment **G** and vorticity **S** at room temperature. The insert shows the polarization vortex in the $x_1 - x_2$ plane when $\mathbf{S} = 0$ at point A. The x_3 axis is outward and parallel to the crystallographic [001] direction.

Fig.2 (Color online) The three-dimensional polarization distributions before (a) and after (b) switching, which corresponds to points B and C in Fig.1, respectively; (c) and (d) are the free energy density distribution in the $x_1 - x_2$ plane for the vortex states (a) and (b), respectively, with the vorticity of S = 0.26 mV/Å^2.

Fig.3 (Color online) Polarization distributions in a nanotube at different normalized evolution times (a) t/t_0=4.0, (b) t/t_0=6.4, (c) t/t_0=6.6, (d) t/t_0=6.8, (e) t/t_0=7.0 and (f) t/t_0=8.0 (t_0 =5.8/*L* ns) under the vorticity of S = 0.26 mV/Å^2, corresponding to the switching from point B to C in Fig.1. Four local vortices, denoted by ellipses in (b), form at the locations where the energy density is the highest as shown in Fig.2 (c). The new and old vortices coexist in (c) as marked by the outer and inner circles, respectively.

Fig.4 (Color online) Evolution of energies (a) and polarizations (b) during the switching from point B to C in Fig.1. In (a), $F = \int_V \psi \, dv$ and other energies are obtained similarly by integrating the corresponding energy densities. In (b), curves denote the averages of absolute values of polarizations.

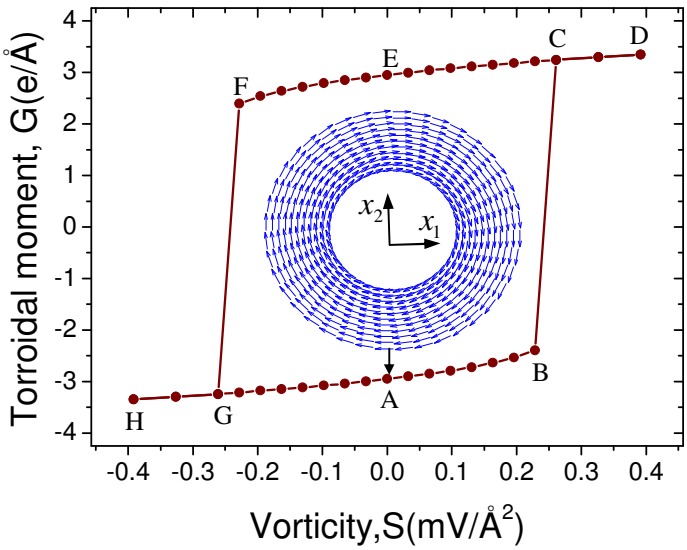

Fig.1 (Color online) The hysteresis loop between the toroidal moment **G** and vorticity **S** at room temperature. The insert shows the polarization vortex in the $x_1 - x_2$ plane when $\mathbf{S} = 0$ at point A. The x_3 axis is outward and parallel to the crystallographic [001] direction.

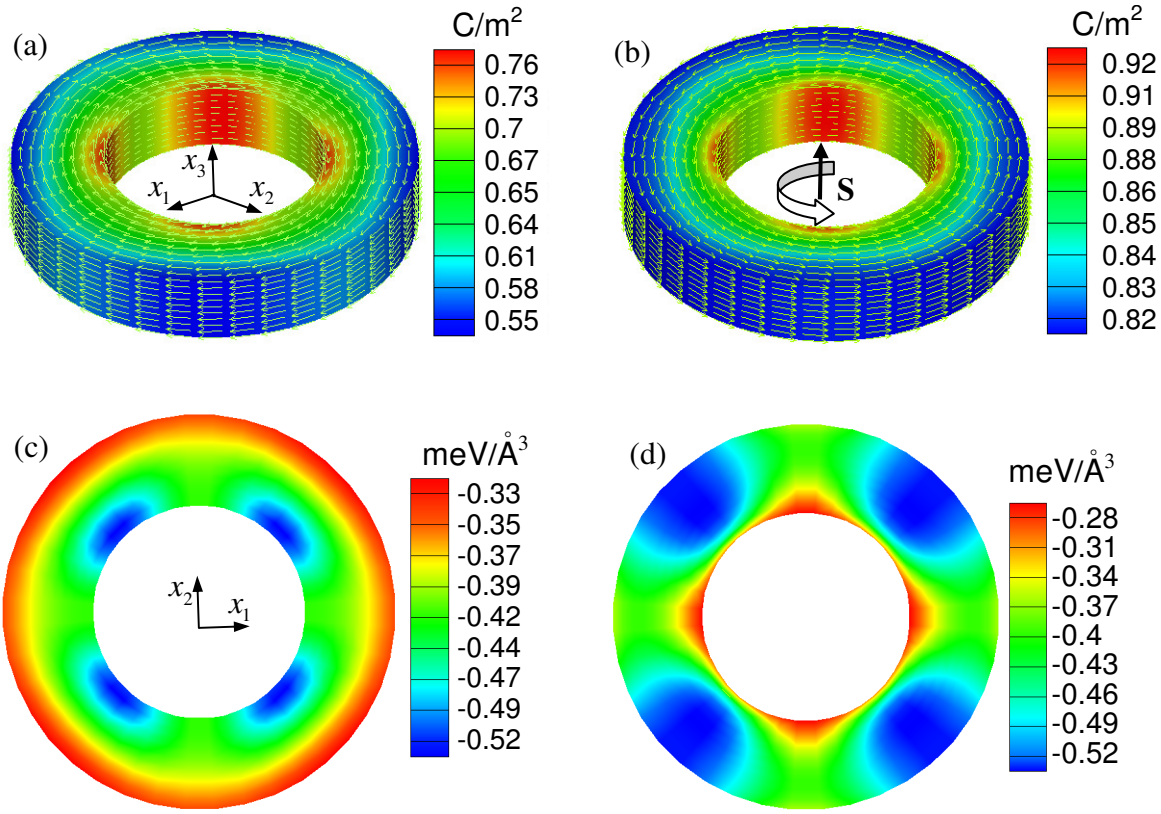

Fig.2 (Color online) The three-dimensional polarization distributions before (a) and after (b) switching, corresponding to points B and C in Fig.1, respectively; (c) and (d) are the free energy density distribution in the $x_1 - x_2$ plane for the vortex states (a) and (b), respectively, under the vorticity of S = 0.26 mV/Å^2.

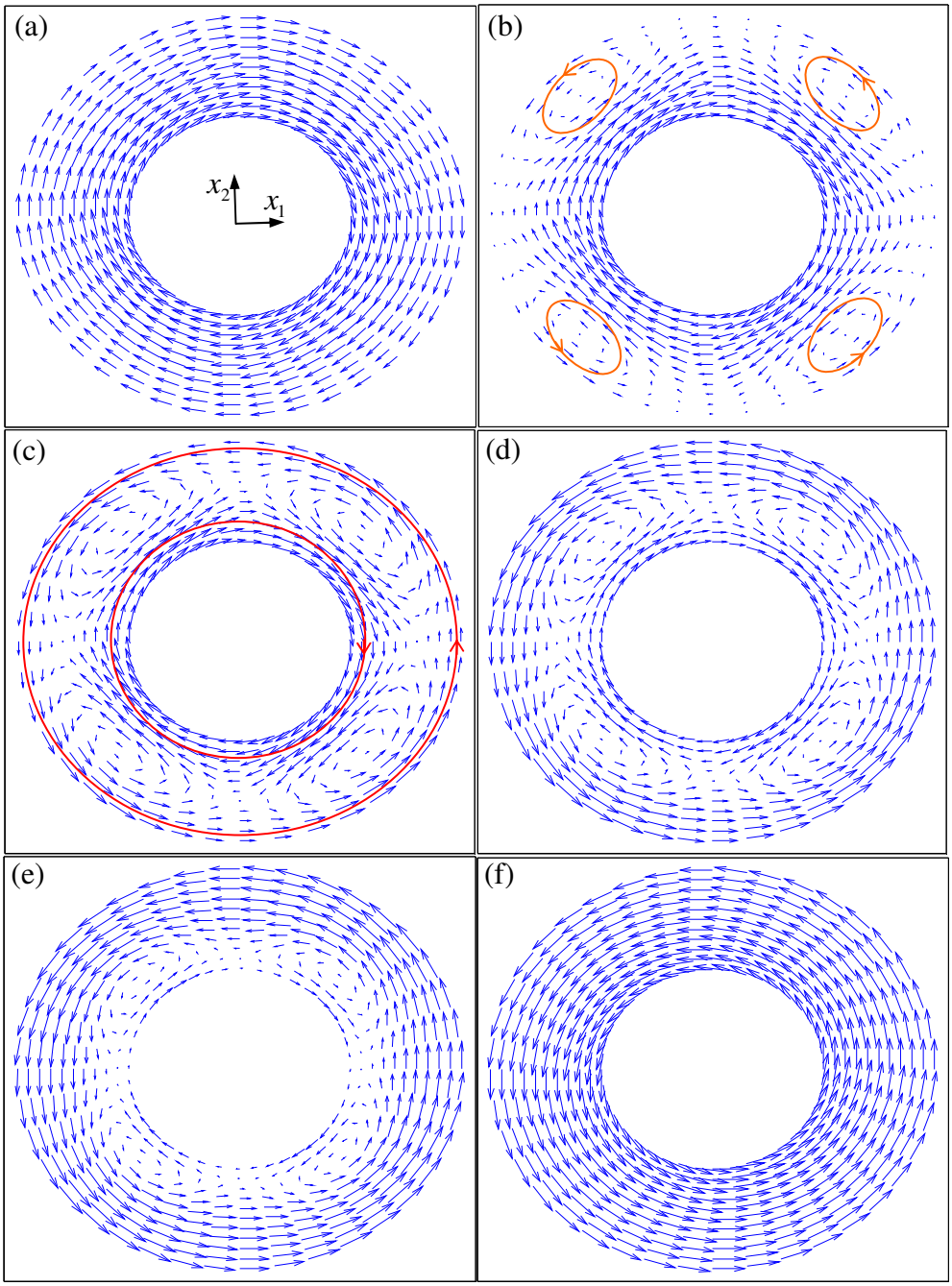

Fig.3. (Color online) Polarization distributions in a nanotube at different normalized evolution times (a) t/t_0=4.0, (b) t/t_0=6.4, (c) t/t_0=6.6, (d) t/t_0=6.8, (e) t/t_0=7.0 and (f) t/t_0=8.0 (t_0 =5.8/L ns) under the vorticity of S = 0.26 mV/Å^2, corresponding to the switching from point B to C in Fig.1. Four local vortices, denoted by ellipses in (b), form at the locations where the energy density is the highest as shown in Fig.2 (c). The new and old vortices coexist in (c) as shown by the outer and inner circles, respectively.

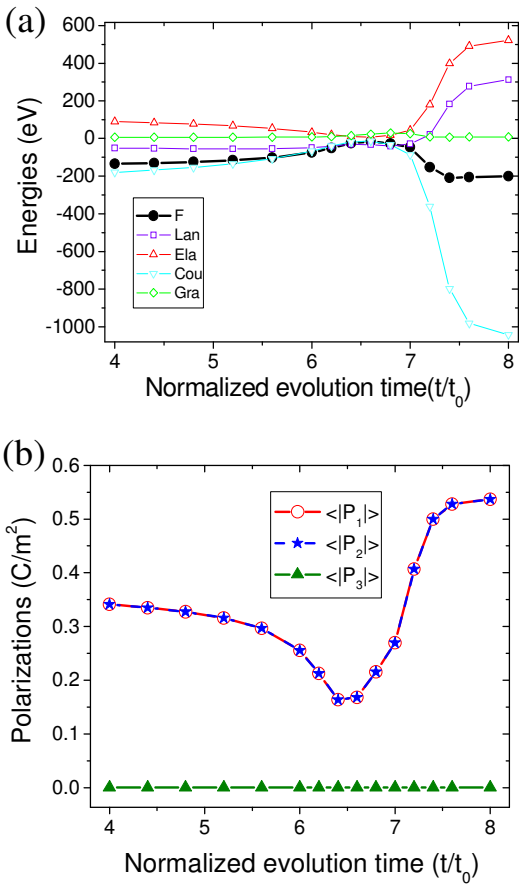

Fig.4. (Color online) Evolution of energies (a) and polarizations (b) during the switching from point B to C in Fig.1. In (a), $F = \int_V \psi \, dv$ and other energies are obtained similarly by integrating the corresponding energy densities. In (b), curves denote the averages of absolute values of polarizations.